INTERNATIONAL JOURNAL FOR NUMERICAL METHODS IN FLUIDS, VOL. 25, 749–778 (1997)

THE SURFACE MARKER AND MICRO CELL METHOD

SHEA CHEN,* DAVID B. JOHNSON,** PETER E. RAAD AND DANI FADDA

Mechanial Engineering Department, Southern Methodist University, Dallas, TX 75275-0337, U.S.A.

SUMMARY

A new method is presented for the simulation of two-dimensional, incompressible, free surface fluid flow problems. The surface marker and micro cell (SMMC) method is capable of simulating transient free surface fluid flow problems that include multivalued free surfaces, impact of free surfaces with solid obstacles and converging fluid fronts (including wave breaking). New approaches are presented for the advection of the free surface, the calculation of the tentative velocity, final velocity and pressure fields and the use of multivalued velocities to treat converging fluid fronts. Simulation results are compared with experimental results for water sloshing in a tank to demonstrate the validity of the new method. Convergence of the new method is demonstrated by a grid refinement study. © 1997 John Wiley & Sons, Ltd.

Int. J. Numer. Meth. Fluids, **25**: 749–778 (1997).

No. of Figures: 14. No. of Tables: 1. No. of References: 9.

KEY WORDS: surface marker; micro cell method

1. INTRODUCTION

The numerical simulation of unsteady, incompressible, free surface fluid flow problems is particularly challenging because the location of the free boundary is not known *a priori* and the temporal evolution of the fluid pressure is not directly described by the governing equations of continuity and momentum. Hence any solution procedure for free surface fluid flow problems must include a method for locating and advancing the free surface as well as for treating the free surface boundary conditions for velocity and pressure. In fact, the capability of any solution procedure is determined to a very significant extent by the method employed for the numerical treatment of the free surface. Additionally, pressure variations within the fluid field play a crucial role in the time evolution of the flow field, especially when relatively rapid changes occur as in the case of impact. Consequently, the solution procedure must not only be capable of calculating the pressure field accurately but must also make provisions to deal with the occurrence of impact, whether between a fluid front and a solid obstacle or between parts of the fluid front itself.

The first method to address the challenges associated with the simulation of free surface fluid flow was the marker and cell (MAC) method, which was published in 1965 by Harlow and Welch[1] and

* Current address: Defense Systems & Electronics Group, Texas Instruments, Dallas, TX, U.S.A.
** Correspondence to: D. B. Johnson, Mechanical Engineering Department, Southern Methodist University, Dallas, TX 75275-0337, U.S.A.

Contract grant sponsor: Defense Advanced Research Projects Agency; Contract grant number: MDA09386-C-0182
Contract grant sponsor: National Science Foundation; Contract grant number: DDM-9114846

CCC 0271–2091/97/070749–30 $17.50
© 1997 by John Wiley & Sons, Ltd.
Received 29 April 1996
Revised 14 November 1996

Welch *et al.*[2] They introduced massless markers that move with the fluid and a novel finite difference solution algorithm for the velocity field. The new method described in this paper is, like the MAC method, a finite difference method that employs massless markers to track the movement of the fluid. The new method is therefore a marker and cell method, but it otherwise differs from the MAC method in essentially every significance respect.

Surface markers,[3] rather than markers distributed throughout the fluid, are used in the SMMC method. New procedures also are used to insure that only physically meaningful velocity information is used to move the surface markers and advect the free surface. Physically motivated new procedures to carefully approximate momentum fluxes, as opposed to straightforward use of finite difference approximations of terms in the Navier–Stokes equations, are used for the calculation of the tentative internal velocity field. To avoid the physically unrealistic use in previous methods of the continuity equation to calculate tentative surface velocities, as well as the resulting inconsistency between the treatments of pressure and continuity in surface and full cells, a new approach also is used for the determination of tentative surface velocities.

In connection with converging fluid fronts, new procedures that incorporate multivalued velocities insure the use of physically relevant information in the calculation of the velocity and pressure fields. In order to appreciate the new procedures for the assignment of appropriate values at different stages in the computational cycle to velocities between converging fluid fronts, it is important to understand that velocities are required in the simulation for three different purposes. First, the final internal velocities from the previous cycle and appropriate velocity boundary conditions are required for marker movement in the current cycle. Second, the final internal velocities from the previous cycle and appropriate velocity boundary conditions are also required for the calculation of the tentative internal velocities in the current cycle. Third, the tentative internal velocities and appropriate velocity boundary conditions are required for the calculation of the incompressibility deviations, which provide the forcing terms in the pressure Poisson equation.

In order to assign appropriate values at different points in the computational cycle to velocities between converging fluid fronts, it is necessary to take into account the physical purpose for which the velocity is intended. For the same velocity one value may be appropriate for a given purpose but inappropriate for a different purpose.

In the SMMC method the assignment of free surface velocity boundary conditions in conjunction with marker movement is governed by mass conservation considerations. During marker movement the final velocity field from the previous cycle, for which the discrete continuity equation is satisfied in each cell, is used to advance the free surface in such a way that fluid is neither gained nor lost. On the other hand, the appropriate transfer of momentum is the primary consideration in the calculation of the tentative velocities in the current cycle. Mass conservation is not the primary consideration, because the tentative velocity field will not, in general, satisfy continuity. Finally, for the calculation of the incompressibility deviation for each cell and the subsequent calculation of the pressure field the primary concern is the development of a physically appropriate pressure field.

The details of the SMMC method are presented in Sections 2–8. First the numerical algorithm and the computational domain of macro and micro cells[4] are described in Section 2. Then the physical justification for and details of new procedures for the evolution of the free surface, for the calculation of tentative velocities, for the assignment of velocities associated with new fluid cells, for the treatment of pressure boundary conditions, for the calculation of final velocities and for the use of multivalued velocities to treat converging fluid fronts are described in Sections 3–8 respectively.

Simulation and experimental results for water sloshing in a tank are compared in Section 9 to demonstrate the validity of the SMMC method. A grid refinement study is presented in Section 10 to demonstrate convergence. Conclusions are stated in Section 11.

 © 1997 John Wiley & Sons, Ltd.

2. THE COMPUTATIONAL FRAMEWORK

The SMMC computational cycle is outlined in Figure 1, where x and y are Cartesian co-ordinates, t is the time, u and v are the x-and the y-component of velocity respectively, $\tilde{u}$ and $\tilde{v}$ are the tentative internal velocities, v is the kinematic viscosity, ρ is the density, g_x and g_y are the components of the acceleration of gravity and p is the pressure. The tentative velocity equations, the incompressible deviation function D, the pressure Poisson equation and the final velocity equations are all shown in Figure 1.

The SMMC computational domain is comprised of macro computational and boundary cells. Micro cells are selectively superimposed on the macro cells in order to obtain a better definition of the location of the free surface than can be achieved by the use of macro cells alone. The micro cells are created by subdividing each macro cell into $N \times N$ micro cells, where N is an odd integer chosen by the analyst. At any given time during a simulation, only micro cells near the free surface are involved in the computations. Surface markers are used to track the movement of the free surface,

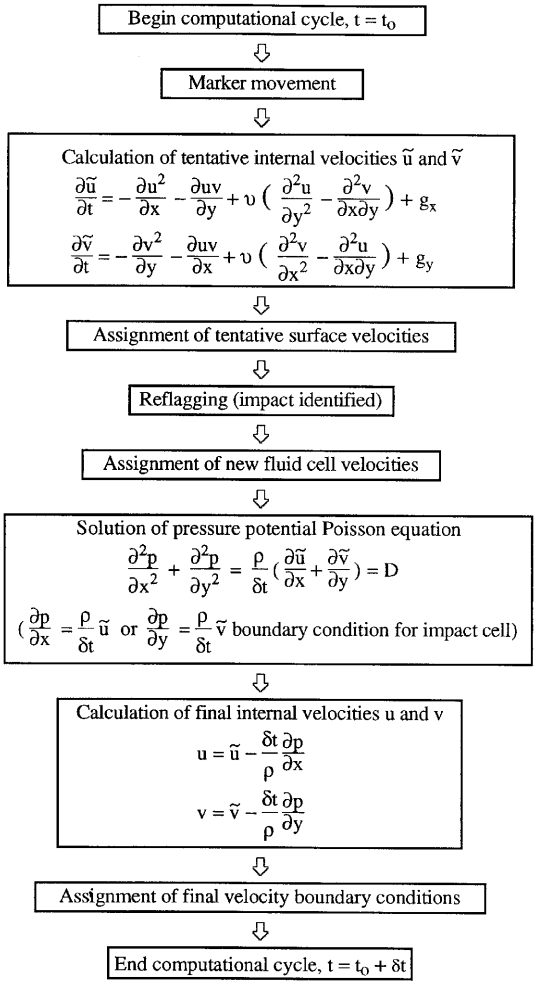

Figure 1. SMMC computational cycle

© 1997 John Wiley & Sons, Ltd.

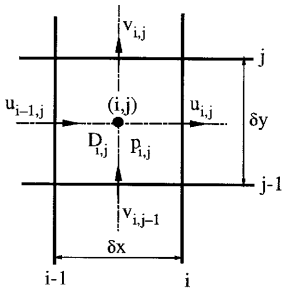

Figure 2. Staggered grid and discrete variables for cell (i, j)

while surface micro cells are used to define the location of the free surface for the application of free surface pressure boundary conditions.

As shown in Figure 2 for a typical macro cell (i, j) of dimensions δx and δy, the staggered grid concept is used to locate the discrete field variables and functions of those variables. The pressure $p(i, j)$ and the incompressibility deviation function $D(i, j)$ are located at the centre of the cell, the discrete velocities $u(i, j)$ and $u(i - 1, j)$ are located at the middle points of the right and left faces respectively and the discrete velocities $v(i, j)$ and $v(i, j - 1)$ are located at the middle points of the top and bottom faces respectively.

Cells are flagged to indicate the presence of fluid. A macro or micro cell that contains any amount of fluid is called a fluid cell and is flagged as either surface or full. The flag of a fluid macro cell is based on the condition of its macro cell neighbours, while the flag of a fluid micro cell is based on the condition of its micro cell neighbours. Otherwise, the definitions of the flags of macro and micro cells are identical. A surface cell is a fluid cell that contains a surface marker and has at least one empty neighbour, while a full cell is defined as a fluid cell that has no empty neighbours. Near the free surface it is possible for a macro cell that contains surface markers to be flagged as a full macro cell. Otherwise, full cells do not contain markers.

The first step in the SMMC computational cycle is the movement of markers. Next the tentative internal velocities at $t_0 + \delta t$ are calculated. An internal velocity is a velocity between fluid cells. Both marker movement and the calculation of tentative velocities are based on information available at the conclusion of the previous cycle, namely on the cell flags at t_0, the internal velocity field at t_0 and the boundary velocities at t_0. The tentative surface velocities in the new computational cycle are assigned immediately following the calculation of the tentative internal velocities. A surface velocity is a velocity between a surface cell and an empty cell. Reflagging occurs only after the determination of the complete tentative velocity field. During reflagging, impact is identified. After reflagging, values are assigned for new fluid cell velocities as required. At this point the fluid configuration at $t_0 + \delta t$ is set and tentative velocities at $t_0 + \delta t$ are known. The influence of pressure on the change in the velocities has until this point not been computed. Now the tentative velocities $\tilde{u}$ and $\tilde{v}$ are used to compute the incompressibility deviation D and the pressure Poisson equation is solved. The pressure and tentative velocities are then used to calculate the final internal velocities. The last step is the assignment of the final surface velocities. At the end of the computational cycle the values of all relevant quantities—the marker positions, the cell flags, the internal velocities, the surface velocities and the pressure—are known at time $t_0 + \delta t$.

3. FREE SURFACE ADVECTION

The evolution of the fluid free surface is accomplished by moving the surface markers to new locations according to

$$x_k^{n+1} = x_k^n + u_k \delta t, \qquad y_k^{n+1} = y_k^n + v_k \delta t, \tag{1}$$

 © 1997 John Wiley & Sons, Ltd.

where the superscripts n and $n+1$ represent time levels and the subscript k represents the marker number. The marker velocity components u_k and v_k are computed by use of an area-weighting scheme. For the marker k shown in Figure 3, the explicit expressions for u_k and v_k are

$$u_k = \frac{A_1 u_1 + A_2 u_2 + A_3 u_3 + A_4 u_4}{\delta x \delta y}, \qquad v_k = \frac{A_5 v_1 + A_6 v_2 + A_7 v_3 + A_8 v_4}{\delta x \delta y}, \tag{2}$$

where the local velocities u_1, u_2, u_3, u_4, v_1, v_2, v_3 and v_4 are final velocities from the preceding computational cycle and A_1 to A_8 are associated weighting areas.

Equations (1) and (2) were first proposed in the original MAC method for use in the movement of markers distributed throughout the fluid. The same equations are used in the SMMC method for the movement of surface markers. When free surfaces converge, however, special care must be exercised in choosing physically appropriate local velocities for use in (2). Otherwise, grossly incorrect results for the movement of the free surfaces can be obtained. In the following, typical situations associated with the approach of free surfaces toward each other are identified and new techniques used in the SMMC method to treat them are presented.

Three typical situations that occur when free surfaces approach each other are shown in Figure 4. At some point during the approach of two free surfaces toward each other, the two free surfaces will be separated by a single empty macro cell as shown in Figure 4(a). According to the area-weighting scheme expressed in (2), the outside tangential velocity $v_{i,j-1}$ shown in Figure 4(a) is a local velocity that is required for the estimation of the y-direction velocity components of both the marker k associated with the free surface on the left and the marker m associated with the free surface on the right.

In previous methods a value is assigned to each outside tangential velocity prior to marker movement and that value is simply used as required for the movement of markers. In general, however, a single value of an outside tangential velocity such as $v_{i,j-1}$ can be meaningful for only one of the free surfaces or the other in a situation such as the one shown in Figure 4(a). As a consequence, if the same value $v_{i,j-1}$ is used to determine the velocities of markers associated with both of the free surfaces, the movement of one of the two surfaces will be distorted, since its movement will be influenced by an unrelated velocity. In addition, the convergence of the free surfaces will be retarded.

In order to avoid the distortion referred to above, a particular velocity such as $v_{i,j-1}$ in Figure 4(a) is a double-valued in the SMMC method. When the movement of a marker such as k that is associated with the fluid on the left in Figure 4(a) is under consideration, $v_{i,j-1}$ is treated as an outside tangential velocity of the fluid on the left and is assigned the value of $v_{i-1,j-1}$ (see Reference 5 for a discussion of the assignment of outside tangential velocities). However, when a marker such as m that is

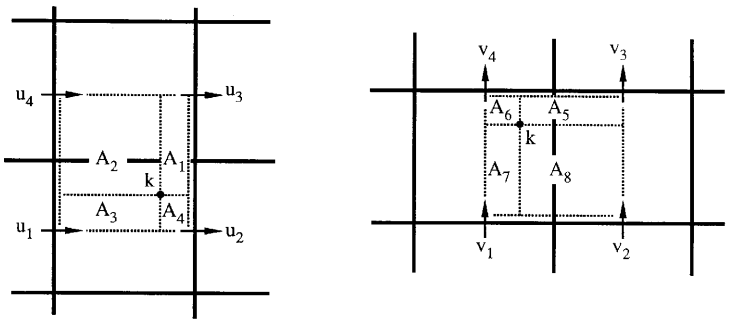

(a) x-component (b) y-component

Figure 3. Area-weighting scheme for marker movement

© 1997 John Wiley & Sons, Ltd.

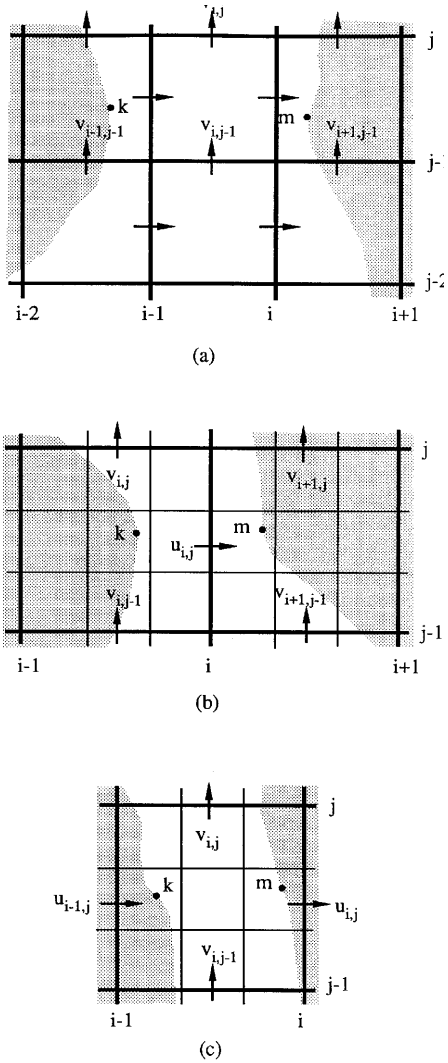

Figure 4. Multivalued velocities employed to move markers

associated with the fluid on the right in Figure 4(a) is under consideration, $v_{i,j-1}$ is treated as an outside tangential velocity of the fluid on the right and is assigned the value of $v_{i+1,j-1}$. Since, unlike in previous methods, outside tangential velocities are not stored in the SMMC method, it does not matter whether marker k is moved before or after marker m. The velocity $v_{i,j}$ in Figure 4(a) is also double-valued in the SMMC method. Since a local velocity such as $v_{i,j}$ or $v_{i,j-1}$, which at the same instant is an outside tangential velocity associated with two different fluid fronts, is evaluated accurately in the SMMC method when the movement of either fluid front is under consideration, the undesired distortion introduced in one of the fluid fronts by use of previous methods is eliminated.

As the two free surfaces shown in Figure 4(a) continue to approach each other, additional difficulties associated with marker movement emerge. At some point the two free surfaces will have moved into adjacent macro cells as shown in Figure 4(b). For the situation shown in Figure 4(b), the velocity $u_{i,j}$ is an internal velocity, since cells (i, j) and $(i+1, j)$ both contain fluid. Although $u_{i,j}$

 © 1997 John Wiley & Sons, Ltd.

technically is an internal velocity which was assigned a final value at the end of the last computational cycle, the fluid fronts located in cells (i, j) and $(i+1, j)$ have not yet come into contact with each other and $u_{i,j}$ is actually located between the two fronts. Therefore the internal velocity $u_{i,j}$ also is one of the local velocities that is required for the estimation of the x-direction velocity components of both the marker k associated with the free surface on the left and the marker m associated with the free surface on the right. In order to properly accommodate these three different uses, the velocity $u_{i,j}$ shown in Figure 4(b) is triple-valued in the SMMC method.

When the movement of marker k in Figure 4(b) is under consideration, the fluid on the right is temporarily ignored and $u_{i,j}$ is treated as a surface velocity of cell (i, j). That is, $u_{i,j}$ is calculated by use of the discrete approximation of the continuity equation associated with cell (i, j). On the other hand, when the movement of marker m is under consideration, the fluid on the left is temporarily ignored and $u_{i,j}$ is treated instead as a surface velocity of cell $(i+1, j)$. Neither of these values of $u_{i,j}$ that is used for marker movement is stored. The stored value of $u_{i,j}$ is the final value that was assigned in the last computational cycle and that contains velocity information from both of the converging fluid fronts. If convergence of the two fluid fronts occurs in the current cycle, this stored value of $u_{i,j}$ is used to calculate incompressibility deviations that allow the determination of the pressures in cells (i, j) and $(i+1, j)$. A thorough discussion of this special case is found in Section 7.

Single values also do not suffice for the velocities $v_{i,j}$, $v_{i+1,j}$, $v_{i,j-1}$ and $v_{i+1,j-1}$ shown in Figure 4(b). For example, $v_{i,j}$ is an outside tangential velocity for the fluid on the right but is at the same time an internal velocity for the fluid on the left. Similar statements apply with respect to velocities $v_{i+1,j}$, $v_{i,j-1}$ and $v_{i+1,j-1}$.

As two free surfaces continue to approach each other, they eventually occupy the same macro cell. In the SMMC method, as long as one empty micro cell exists between the converging fluid fronts, the motion of one front does not affect the motion of the other. It is possible, as shown in Figure 4(c), for an empty micro cell to exist between two free surfaces found in the same macro cell. The philosophy associated with the calculation of the x-direction velocities u_k and u_m of markers k and m in Figure 4(c) is the same as that associated with the calculation of the velocities of markers on the converging free surfaces shown in Figures 4(a) and 4(b). Specifically, when marker k in Figure 4(c) is under consideration, the fluid on the right is ignored, $u_{i-1,j}$ is treated as an internal velocity of the fluid on the left, $v_{i,j}$ and $v_{i,j-1}$ are assigned as outside tangential velocities of the fluid on the left and $u_{i,j}$ is assigned as a surface velocity. On the other hand, when marker m is under consideration, the fluid on the left is ignored, $u_{i,j}$ is treated as an internal velocity of the fluid on the right, $v_{i,j}$ and $v_{i,j-1}$ are assigned as outside tangential velocities of the fluid on the right and $u_{i-1,j}$ is assigned as a surface velocity.

In the SMMC method, velocities that serve different purposes in connection with the convergence of two fluid fronts are multivalued. The use of multivalued velocities eliminates the distortion caused by the inappropriate use of a single value for certain local velocities that influence the movement of two different fluid fronts. The value used for each local velocity required for the computation of the velocity of a surface marker is always appropriate for the fluid front under consideration.

4. TENTATIVE VELOCITIES

In each computational cycle, tentative velocities are either calculated by use of the simplified Navier–Stokes equations in which the pressure terms have been neglected, or assigned by use of the best available velocity information. Different procedures are required for internal as opposed to surface velocities. The appropriate transfer of momentum is the primary physical consideration for the calculation of a tentative internal velocity. The details of physically motivated new procedures to calculate momentum fluxes are presented in this section. It is observed that the use of standard finite

© 1997 John Wiley & Sons, Ltd.

difference approximations can lead to physically erroneous momentum flux values in certain situations. Momentum transfer considerations cannot be used, however, for the determination of a tentative surface velocity, since the associated control volume is not even within the fluid. In previous methods the continuity equation has been applied to the surface cells to compute the surface velocities, in spite of the fact that the surface cells are not full and that the continuity equation may not be satisfied in any other cells at this stage of the computational cycle. An entirely new approach based on the use of physically relevant neighbouring acceleration information is used in the SMMC method for the computation of tentative surface velocities.

When standard finite difference approximations are used either of the simplified Navier–Stokes equations or of the pressure Poisson equation, it is implicity assumed that the control volume associated with each velocity or pressure is full of fluid. The control volumes for the computations of the tentative velocities $u_{i,j}$ and $v_{i,j}$ and of the pressure $p_{i,j}$ are shown in Figure 5. For a control volume that lies entirely within the fluid-filled region, the assumption that the control volume is full of fluid is valid. In general, however, this assumption is not valid for a control volume near the free surface. In particular, when free surfaces converge, the control volumes associated with some of the internal velocities in the neighbourhood of the free surface may even be almost entirely empty.

A typical situation associated with converging free surfaces is shown in Figure 6. For the configuration shown in Figure 6, cell $(i+1, j)$ is the only empty macro cell, cells $(i+2, j)$, $(i+1, j+1)$, (i, j) and $(i+1, j-1)$ are surface cells and all the other macro cells are full. Referring to Figure 6, none of the control volumes associated with the 14 internal velocities $u_{i+2,j+1}$, $u_{i+1,j+1}$, $u_{i,j+1}$, $u_{i-1,j}$, $u_{i-1,j-1}$, $u_{i,j-1}$, $u_{i+1,j-1}$, $u_{i+2,j}$, $v_{i+2,j+1}$, $v_{i+1,j+1}$, $v_{i,j}$, $v_{i,j-1}$, $v_{i+2,j-1}$ and $v_{i+2,j}$ is full of fluid. The extreme cases are $v_{i+1,j+1}$ and $v_{i+2,j}$. The control volume associated with $v_{i+1,j+1}$ is almost completely full, while the control volume associated with $v_{i+2,j}$ is almost completely empty. The amounts of fluid contained in the control volumes associated with the other 12 velocities that have been identified are between these extremes. In the new method, special treatments are employed to determine appropriate values of the tentative velocities associated with cells near the free surface.

The new procedures presented in the remainder of this section enable the successful simulation of free surface fluid flow problems that include converging fluid fronts. Five new procedures are discussed separately. Micro cells play an essential role in the implementation of these procedures. First, the procedure used to determine whether a tentative value for a given internal velocity will be calculated by use of the simplified Navier–Stokes equations or, instead, will be assigned is discussed in Section 4.1. Second, the general approach used for the calculation of tentative internal velocities is explained in Section 4.2. Third, the special procedures required for calculating tentative velocities associated with converging fluid fronts are presented in Section 4.3. Fourth, the procedures used in certain special situations to assign tentative internal velocities by use of the best available information are described in Section 4.4. Fifth, new procedures for the determination of tentative surface velocities are presented in Section 4.5.

4.1. Decision to calculate a tentative internal velocity

In previous methods the simplified Navier–Stokes equations are used to calculate a tentative value for each internal velocity, i.e. for each velocity associated with a face that is shared by two macro cells that contain fluid. In the new method, however, the simplified Navier–Stokes equations are not used to calculate values for certain internal velocities. Consequently, for a particular internal velocity the first step is to make a decision whether or not to calculate a tentative value by use of the simplified Navier–Stokes equations. If the internal velocity in question is located outside the fluid, no tentative velocity is calculated. Instead, tentative values for such internal velocities are assigned by use of the most physically meaningful information as described in Section 4.4.

 © 1997 John Wiley & Sons, Ltd.

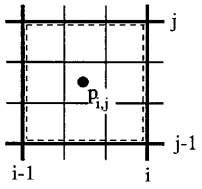

(a) The Control Volume for Pressure $p_{i,j}$

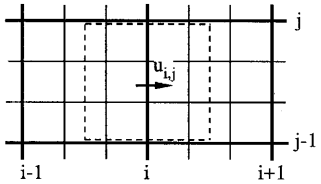

(b) The Control Volume for Velocity Component $u_{i,j}$

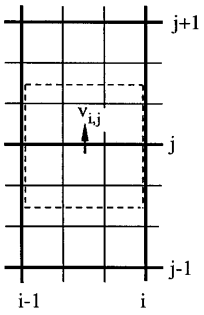

(c) TheControl Volume for Velocity Component $v_{i,j}$

Figure 5. Control volumes

Associated with each macro cell that contains fluid are neighbouring points e, n, w and s located to the east, north, west and south respectively of the centre of the cell. Each of these points is either the centre of an adjacent macro cell or the centre of a surface micro cell. The distances between the centre of the macro cell under consideration and points e, n, w and s are designated le, ln, lw and ls respectively and are referred to as leg lengths. If the centre micro cell of a given macro cell is not full, then all four leg lengths are equal to zero for that macro cell. At the other extreme, $le = lw = \delta x$ and $ln = ls = \delta y$ if the macro cell under consideration is full and all four of its macro cell neighbours are also full. If a fluid free surface exists between the centre of the macro cell and the centre of one of its neighbours, then le, lw, ln or ls may be as small as zero or as large as δx or δy, depending on the location of the free surface. Micro cells enable the efficient determination of leg lengths and leg length information enables the straightforward identification of internal velocities that lie outside the fluid.

Referring to Figure 6, $v_{i,j-1}$ and $v_{i+2,j}$ both are internal velocities, since each velocity is located on a face shared by a surface cell and a full cell. That both of them are also located outside the fluid is

© 1997 John Wiley & Sons, Ltd.

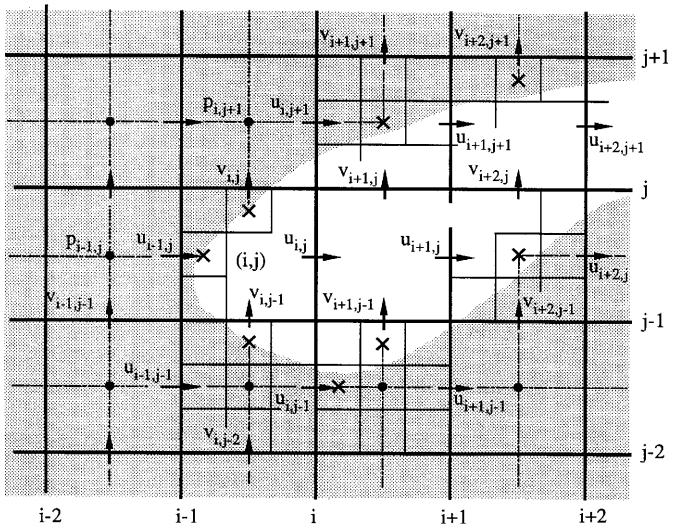

Figure 6. Internal velocities near free surface

determined by examination of leg length values. For example, since $ls_{i,j}$ and $ln_{i,j-1}$ are both less than $\delta y/2$ (in this case, $ls_{i,j} = 0$ and $ln_{i,j-1} = \delta y/3$), $v_{i,j-1}$ lies outside the fluid. Furthermore, since $ls_{i+2,j+1} = ln_{i+2,j} = 0$, $v_{i+2,j}$ also lies outside the fluid. Consequently, no tentative value is calculated for either of these two velocities.

4.2. General procedure for calculation of tentative internal velocities

By use of the Gauss theorem the integrated value of the momentum flux terms in the Navier–Stokes equations over the control volume can be converted to the value of the momentum flux across the boundary of the control volume. In general, the calculation of tentative internal velocities in the new method is accomplished by making use of the best available information in a particular situation to carefully approximate the momentum flux across each face of the appropriate control volume, as opposed to the straightforward use of standard finite difference approximations of the terms in the simplified Navier–Stokes equations. Consequently, the flux leaving one control volume is automatically gained by the adjacent control volume and momentum conservation is guaranteed.

Even when the region surrounding the tentative velocity in question is completely filled with fluid, there is a difference between the use of the new method and the use of standard finite difference approximations. If, as discussed below, the velocities on opposite faces of a given control volume happen to have opposite signs, the difference is significant. In such a case an incorrect rate of momentum transfer across the faces of the control volume is associated with the use of a standard finite difference approximation. In other cases involving full control volumes, the new approximations are identical with second-order central difference approximations.

The continuous form of the simplified Navier–Stokes equation that governs the tentative acceleration $\partial\tilde{u}/\partial t$ can be written as

$$\frac{\partial \tilde{u}}{\partial t} = -\frac{\partial u^2}{\partial x} - \frac{\partial uv}{\partial y} + v\left(\frac{\partial^2 u}{\partial x^2} + \frac{\partial^2 u}{\partial y^2}\right) + g_x \tag{3}$$

 © 1997 John Wiley & Sons, Ltd.

and the tentative velocity $\tilde{u}$ is calculated according to

$$\tilde{u} = u + \delta t \frac{\partial \tilde{u}}{\partial t}. \tag{4}$$

Similar equations are used to calculate the tentative acceleration $\partial \tilde{v}/\partial t$ and the tentative velocity $\tilde{v}$. The procedures for approximating the first two terms on the right-hand side of (3) will be discussed in detail.

For a particular discrete internal velocity $u_{i,j}$ a tentative value $\tilde{u}_{i,j}$ is calculated by use of (3) and (4) provided that either $le_{i,j}$ or $lw_{i+1,j}$ is larger than $\delta x/2$, which insures that $u_{i,j}$ is inside the fluid region. Otherwise, a tentative value is assigned as described in Section 4.4.

The rate of x-momentum increase (per unit mass) in the control volume as a result of convection across the vertical faces, $-\partial u^2/\partial x$, is calculated by use of the equation

$$-\frac{\partial u^2}{\partial x} \approx \frac{T_L - T_R}{\delta x}, \tag{5}$$

where $T_L/\delta x$ and $T_R/\delta x$ represent the rates of x-momentum transfer across the left and right faces of the control volume respectively. As shown in Figure 5(b), the left and right faces of the control volume are vertical lines passing through the centres of cells (i, j) and $(i+1, j)$ respectively. The problem now is to approximate the rate of x-momentum transfer. Since the calculation of T_R is similar to that of T_L, only the calculation of T_L is described in detail.

The value of T_L is estimated by use of

$$T = \max[U_L U_{DL}, 0], \tag{6}$$

where U_L is the average velocity in the x-direction at the left control face and U_{DL} is the average velocity in the x-direction of the fluid in the donor control volume. Since the x-momentum transfer across the left face of the control volume is always positive, T_L cannot be less than zero. Across the left face, either negative x-momentum is leaving the control volume or positive x-momentum is entering. In either case the x-momentum associated with the control volume is increased by the momentum transfer across its left face. The approximation for U_L is simply given by

$$U_L = \frac{u_{i-1,j} + u_{i,j}}{2}$$

and the sign of U_L determines the donor control volume and therefore the appropriate value for U_{DL}. If U_L is positive, the fluid is flowing from left to right and

$$U_{DL} = u_{i-1,j}.$$

Otherwise, the fluid is flowing from right to left, in which case

$$U_{DL} = u_{i,j}.$$

This efficient new procedure makes use of the best available information to provide an estimate of the increase in x-momentum in the control volume as a result of convection across the vertical faces.

Miyata[6] and Nichols[7] discuss different finite difference approximations of $\partial u^2/\partial x$. The upstream finite difference approximation employed by Hirt and Nichols in their volume of fluid method is similar to the new method presented here, but there is one important difference. In the new method presented here, care is taken to insure that a negative value is never calculated for the rate of momentum transfer across the left face of the control volume. Consequently, T_L is set equal to zero if $U_L U_{DL}$ is negative, which is the case only when $u_{i,j} > 0$ and $u_{i-1,j} < 0$. As a result, a physically incorrect approximation of momentum transfer is avoided in such situations, which can occur even in a region that is completely filled with fluid. Focusing attention on the momentum transfer across the

© 1997 John Wiley & Sons, Ltd.

faces of the control volume rather than on the form of the finite difference approximation of $\partial u^2/\partial x$ led to this improvement.

The rate of increase in x-momentum as a result of convection across the horizontal faces of the control volume, which corresponds to the term $-\partial uv/\partial y$, is calculated by use of the equation

$$-\frac{\partial uv}{\partial y} = \frac{T_B - T_T}{\delta y}, \tag{7}$$

where $T_B/\delta y$ and $T_T/\delta y$ represent the rates of x-momentum transfer across the bottom and top faces of the control volume respectively. As shown in Figure 5(b), the bottom and top faces of the control volume are coincident with the horizontal grid lines $j-1$ and j respectively. Since the calculation of T_T is similar to that of T_B, only the calculation of T_B is described in detail.

The value of T_B is estimated by use of

$$T_B = \frac{V_{BL}U_{DBL} + V_{BR}U_{DBR}}{2}, \tag{8}$$

where $V_{BL} = v_{i,j-1}$ and $V_{BR} = v_{i+1,j-1}$ represent the average velocities in the y-direction along the left and right halves of the bottom face of the control volume for $u_{i,j}$ respectively and U_{DBL} and U_{DBR} represent the average velocities in the x-direction in the appropriate donor control volumes for the left and right halves of the bottom face respectively. The details of the evaluation of $V_{BL}U_{DBL}$ are presented below; $V_{BR}U_{DBR}$ is evaluated in a similar manner.

When either $ls_{i,j}$ or $ln_{i,j-1}$ is larger than $\delta y/2$, the left half of the bottom face of the control volume is immersed in fluid and $V_{BL}U_{DBL}$ is determined as follows. If V_{BL} is positive, the fluid is moving upwards across the left half of the bottom control face, the donor control volume is the control volume associated with $u_{i,j-1}$ and therefore $U_{DBL} = u_{i,j-1}$. On the other hand, if V_{BL} is negative, the fluid is moving downwards; the donor control volume is the control volume associated with $u_{i,j}$ and therefore $U_{DBL} = u_{i,j}$. If V_{BL} is zero, it is not necessary to determine U_{DBL}, since the product of V_{BL} and U_{DBL} is zero regardless of the value of U_{DBL}.

In certain situations no benefit is obtained by considering the left and right halves of the bottom face of the control volume separately. For example, if $ls_{i,j}$ and $ls_{i+1,j}$ are both larger than $\delta y/2$ and furthermore, $v_{i,j-1}$ and $v_{i+1,j-1}$ are both positive, then, by use of (8), T_B can be written as

$$T_B = \frac{v_{i,j-1} + v_{i+1,j-1}}{2}u_{i,j-1},$$

since $U_{DBL} = U_{DBR} = u_{i,j-1}$. This same result obviously can be obtained in a very straightforward manner simply by multiplying the average value of the vertical velocity on the bottom face of the control volume by the horizontal velocity of the donor control volume.

In other situations, however, it is very important to treat the left and right sides of the bottom face of the control volume independently. For example, if $v_{i,j-1}$ is negative and $v_{i+1,j-1} = -v_{i,j-1}$, then the value of T_B calculated by use of (8) can be written as

$$T_B = \frac{v_{i,j-1}u_{i,j} + v_{i+1,j-1}u_{i,j-1}}{2} = \tfrac{1}{2}v_{i,j-1}(u_{i,j} - u_{i,j-1}),$$

which will result in a zero value of T_B only if $u_{i,j} = u_{i,j-1}$. On the other hand, since the average vertical velocity on the bottom face is zero when $v_{i,j-1}$ and $v_{i+1,j-1}$ are equal and opposite, the approach of multiplying the average value of the vertical velocity on the bottom face of the control volume by the horizontal velocity of the donor control volume will always result in a zero estimate of T_B regardless of the values of $u_{i,j}$ and $u_{i,j-1}$. Therefore the use of the new procedure leads to a significantly improved estimate of the momentum convection across the horizontal faces of the

 © 1997 John Wiley & Sons, Ltd.

control volume in such situations, as well as in similar situations that occur in connection with flow over an obstacle and with converging fluid fronts.

When both $ls_{i,j}$ and $ln_{i,j-1}$ are smaller than $\delta y/2$, the left half of the bottom face of the control volume is not immersed in the fluid. Therefore $u_{i,j}$ is used as the donor velocity U_{DBL} regardless of whether V_{BL} is positive or negative. Since there is a gap between the fluid above and below the left half of the bottom face of the control volume, the velocity $u_{i,j-1}$ is not used as the donor velocity even if V_{BL} is positive.

The viscous forces associated with the term

$$v\left(\frac{\partial^2 u}{\partial x^2}+\frac{\partial^2 u}{\partial y^2}\right)$$

are treated as external forces that act on the faces of the control volume. Since the effects of these forces on the rate of increase in x-momentum in the control volume have nothing to do with the mass flow directions, the identification of appropriate donor cells is not necessary. The approximation of this term used in the new method is identical with the approximation obtained by use of standard central difference formulae.

4.3. Converging fluid fronts

Special care must be exercised in the determination of the momentum flux across a face of the control volume in connection with converging fluid fronts. Consider, for example, the calculation of the tentative velocity $\tilde{u}_{i,j}$ for the situation shown in Figure 7. Assume, furthermore, that the general motion of the fluid in Figure 7 is from left to right. If the fluid shown in the left half of Figure 7 were not present, the velocity $u_{i-1,j}$ would represent a surface velocity that is directly related to the movement of the fluid in the control volume associated with $u_{i,j}$. Then, according to the procedure described in the preceding subsection, it would be appropriate to use $u_{i-1,j}$ as the value of U_{DL} in the calculation of the rate of x-momentum transfer, $T_{\mathrm{L}}/\delta x$, across the left face of the control volume. However, owing to the presence of the fluid in the left half of Figure 7, cell $(i-1, j)$ is not empty and $u_{i-1,j}$ is not a surface velocity. For the situation shown in Figure 7, $u_{i-1,j}$ is not directly related to the motion of the fluid in the control volume for $u_{i,j}$. Consequently, $u_{i-1,j}$ is not a physically appropriate donor velocity for momentum transfer across the left face of the control volume. The best available velocity information in this situation is provided by $u_{i,j}$ itself. Therefore both U_{L} and U_{DL} are assigned the value of $u_{i,j}$ in this special situation, resulting in

$$T_{\mathrm{L}} = U_{\mathrm{L}} U_{\mathrm{DL}} = (u_{i,j})^2.$$

A very simple test, enabled by the use of micro cells, reveals the existence of a situation of the type described in this subsection. If $u_{i-1,j}$ is not a surface velocity and either $le_{i,j}$ or $lw_{i,j}$ is less than $\delta x/2$, then a gap exists in the fluid between $u_{i-1,j}$ and $u_{i,j}$ and the special procedure described in this subsection is used for the calculation of the tentative velocity $\tilde{u}_{i,j}$.

For example, in the calculation of the particular tentative velocity $v_{i+2,j-1}$ in Figure 6 an estimate is required of the y-momentum flux across the top face of the control volume. Since cell $(i+2, j+1)$ is not empty, $v_{i+2,j}$ is not a surface velocity. Since, in addition, $ln_{i+2,j} = 0$, the procedure of thi subsection applies and T_{T} is estimated as

$$T_{\mathrm{T}} = V_{\mathrm{T}} V_{\mathrm{DT}} = (v_{i+2,j-1})^2.$$

The ability afforded by the use of micro cells to efficiently identify such situations associated with converging fluid fronts is the key to the development of the new procedures.

© 1997 John Wiley & Sons, Ltd.

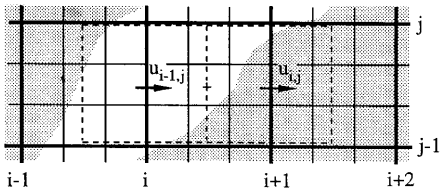

Figure 7. Converging fluid fronts

4.4. Assignment

Even though tentative values are not calculated by use of the simplified Navier–Stokes equations for velocities between fluid cells if the velocities are located outside the fluid, it is necessary for a value to be assigned if the velocity in question is associated with a cell in which the pressure will be calculated. This assignment is necessary so that an incompressibility deviation D can be calculated for the cell in question.

The velocity $v_{i,j-1}$ in Figure 6 is a velocity that is in this category. First, it is a velocity that is located on a face shared by a full cell and a surface cell. Second, it also is located outside the fluid. Consequently, as stated in Section 4.1, a tentative value is not calculated. Third, since cell $(i, j-1)$ is a cell in which pressure will be calculated, a value for the incompressibility deviation $D_{i,j-1}$ is required. Therefore, even though it was not appropriate to calculate a tentative value for $v_{i,j-1}$ by use of the modified Navier–Stokes equations because it is outside the fluid, it is necessary to make use of the best available information to assign a tentative value to $v_{i,j-1}$ for use in the calculation of $D_{i,j-1}$. The new procedure for the assignment of a tentative value to $v_{i,j-1}$ is discussed in the following.

Each discrete velocity has, in general, four neighbours of the same type. The neighbours to the east, south, west and north of $v_{i,j-1}$ are $v_{i+1,j-1}$, $v_{i,j-2}$, $v_{i-1,j-1}$ and $v_{i,j}$ respectively. To determine whether or not one of these neighbour velocities is appropriate for use in the assignment of $v_{i,j-1}$, two questions must be answered. First, is the neighbour velocity in question a fluid velocity that has been calculated by use of the simplified Navier–Stokes equations? If the answer is no, the neighbour velocity is not given any further consideration. If the answer to the first question is yes, the second question must be answered. Is there a fluid path that connects the control volume associated with the neighbour velocity to the control volume associated with $v_{i,j-1}$? If the answer to this second question is no, the neighbour velocity is not physically relevant for use in the assignment of a value to $v_{i,j-1}$. If the answer to the second question is yes, the neighbour velocity under consideration is relevant and will be used in the assignment of $v_{i,j-1}$. The same two questions must be asked in connection with each of the four neighbours of $v_{i,j-1}$. Finally, the value assigned to $\tilde{v}_{i,j-1}$ is the average of the neighbour velocities that have been determined to be relevant.

Micro cells play a central role in the determination of the answer to question two referred to above. The three neighbour velocities south, west and north of $v_{i,j-1}$ all are fluid velocities, while the neighbour velocity east of $v_{i,j-1}$ is not. Consequently, question two is only asked in connection with the neighbour velocities $v_{i,j-2}$, $v_{i-1,j-1}$ and $v_{i,j}$. To determine whether the fluid in the control volume associated with $v_{i,j-2}$ is connected with that in the control volume of $v_{i,j-1}$, the value of the leg length $ln_{i,j-1}$ is checked. If $ln_{i,j-1} > 0$, then the fluid in the two control volumes is connected, and $v_{i,j-2}$ is a relevant velocity. Since $ln_{i,j-1} = \delta y/3$ for the situation shown in Figure 6, $v_{i,j-2}$ is a relevant velocity. To determine whether the fluid in the control volume associated with $v_{i-1,j-1}$ is connected with that in the control volume of $v_{i,j-1}$, it is necessary to check both of the leg lengths $le_{i-1,j}$ and $le_{i-1,j-1}$. If either of these leg lengths is greater than $\delta x/2$, then $v_{i-1,j-1}$ is a relevant velocity. For the specific case shown in Figure 6, $le_{i-1,j} = 2\delta x/3$ and $le_{i-1,j-1} = \delta x$, so $v_{i-1,j-1}$ also is a relevant

 © 1997 John Wiley & Sons, Ltd.

velocity. Finally, to determine the relevance of $v_{i,j}$, it is necessary to check the leg length $ls_{i,j}$. Since $ls_{i,j} = 0$, there is a gap in the fluid between the control volumes associated with $v_{i,j}$ and $v_{i,j-1}$. Consequently, $v_{i,j}$ is irrelevant and the value assigned to $\tilde{v}_{i,j-1}$ is

$$\tilde{v}_{i,j-1} = \frac{\tilde{v}_{i,j-2} + \tilde{v}_{i-1,j-1}}{2}.$$

4.5. *Tentative surface velocities*

After all the tentative internal velocities have been determined, the tentative surface velocities must be determined. Tentative surface velocities are required for the assignment of new fluid cell velocities, for the estimation of impact pressure boundary conditions and for the computation of the incompressibility deviation D for each surface cell in which the pressure will be computed.

As discussed in Sections 4.2 and 4.3, tentative internal velocities are calculated in the new method by carefully approximating the momentum flux across the faces of the appropriate control volume. Momentum flux approximations are not used in the new method, however, to determine tentative surface velocities. Tentative surface velocities also are not computed by use of the continuity equation for each surface cell as in previous methods. Instead, tentative surface velocities are determined by making use of the best available neighbouring acceleration information. As a result, the incompressibility deviation D in a surface cell is not necessarily equal to zero, in contrast with previous methods. This has an important consequence in a surface cell whose centre micro cell is full.

The pressure at the centre of a surface cell whose centre micro cell is full is calculated by use of the pressure Poisson equation. Cell $(i+1, j-1)$ in Figure 6 is an example of a surface macro cell whose centre micro cell is full. Consequently, even though cell $(i+1, j-1)$ is a surface cell, the pressure $p_{i+1,j-1}$ is calculated by use of the pressure Poisson equation. Prior to the calculation of $p_{i+1,j-1}$ the surface velocity $v_{i+1,j-1}$ is assigned and the incompressibility deviation $D_{i+1,j-1}$ is computed. The outcome is that an appropriate pressure $p_{i+1,j-1}$ is calculated. This pressure later is used in the calculation of final internal velocities. Only after the final internal velocities have been adjusted for the effects of pressure to insure that continuity is satisfied in the full cells are the final surface velocities computed to insure that continuity is satisfied in the surface cells as well. Micro cells enable the identification of a surface cell of this type, the application of the free surface pressure boundary condition at a point or points near the free surface within the cell and the efficient and accurate calculation of the pressure at the centre of the surface cell.

There is a fundamental difference between the approach used in the new method and that used in previous methods. When, as in previous methods, the continuity equation is used to compute a tentative surface velocity and the pressure in the surface cell is set equal to zero or to some other constant prior to the solution of the pressure Poisson equation, the effects of pressure in the surface cell are expressly being taken into account. In general, however, continuity is not satisfied in the full cells by the tentative internal velocities and the explicit purpose of the determination of the pressure field and the subsequent calculation of the final velocities is to satisfy continuity and take into account the effects of pressure, which were not taken into account in the determination of the tentative internal velocities. As a result, there is an inconsistency in previous methods between the way in which pressure and continuity are treated in the surface cells as opposed to the full cells. In a surface cell, pressure is taken into account and the continuity equation is satisfied prior to the calculation of the pressure field, while in the full cells, pressure effects are not taken into account and the continuity equation is not satisfied until after the pressure field has been calculated. In the new method, however, in all cells, both surface and full, pressure effects are not taken into account and the continuity equation is not satisfied until after the determination of the pressure field.

© 1997 John Wiley & Sons, Ltd.

The basic features of the new method for the determination of a tentative surface velocity such as $\tilde{u}_{i,j}$ are that the tentative surface acceleration $\partial\tilde{u}_{i,j}/\partial t$ is first assigned a value, followed by the calculation of $\tilde{u}_{i,j}$ according to

$$\tilde{u}_{i,j} = u_{i,j} + \delta t \frac{\partial \tilde{u}_{i,j}}{\partial t}. \tag{9}$$

If $u_{i,j}$ is a surface velocity, then either cell (i, j) or cell $(i+1, j)$ must be an empty cell. If cell (i, j) is an empty cell and cell $(i+1, j)$ is a surface cell, then the acceleration $\partial\tilde{u}_{i+1,j}/\partial t$ is the most appropriate information for use in estimating the tentative surface velocity $\tilde{u}_{i,j}$. Therefore

$$\frac{\partial \tilde{u}_{i,j}}{\partial t} = \frac{\partial \tilde{u}_{i+1,j}}{\partial t}.$$

That is, the change in the surface velocity $u_{i,j}$ as a result of the inertial, viscous and gravitational forces is estimated to be the same as the change in $u_{i+1,j}$, the closest fluid velocity. The tentative surface velocity $\tilde{u}_{i,j}$ is then calculated by use of (9).

If, on the other hand, cell $(i+1, j)$ is an empty cell and cell (i, j) is a surface cell, as is the case in Figure 6, then the acceleration $\partial\tilde{u}_{i-1,j}/\partial t$ is the most appropriate information for use in estimating the tentative surface velocity $\tilde{u}_{i,j}$, so that

$$\frac{\partial \tilde{u}_{i,j}}{\partial t} = \frac{\partial \tilde{u}_{i-1,j}}{\partial t}.$$

It is possible that both cell $(i-1, j)$ and cell $(i+1, j)$ are empty cells. This will be true when there is a thin strip of fluid extending vertically through cell (i, j). In this case there is no neighbouring acceleration that is calculated by use of the Navier–Stokes equation. The only acceleration information that is available is the acceleration due to gravity. Therefore the time rate of change in $\tilde{u}_{i,j}$ that is due to effects other than pressure is simply approximated in this case according to

$$\frac{\partial \tilde{u}_{i,j}}{\partial t} = g_x.$$

The new tentative surface velocity assignment method is physically meaningful, logically simple and computationally efficient. Most importantly, it makes possible the use of a consistent method to compute the pressure field in each macro cell whose centre micro cell is full.

The method used for the determination of tentative surface velocities affects the changes that occur in both the pressure and velocity fields during any time increment in any free surface fluid flow problem. For certain time increments the difference between the use of different methods for the determination of tentative surface velocities can be very dramatic. If, for example, impact occurs during the time increment under consideration, the new method enables the determination of the pressure pulse associated with the impact and of its effects, whereas the use of a method in which the continuity equation is satisfied and the pressure is assigned in a surface cell prior to the solution of the pressure Poisson equation precludes the possibility either of determining or of taking into account the pressure pulse associated with the impact.

5. TENTATIVE NEW FLUID CELL INTERNAL VELOCITIES

New fluid cells are created during a computational cycle by the movement of markers into cells that did not contain fluid at the start of the cycle. As a result, a discrete velocity on the face of such a cell can suddenly become an internal velocity and no velocity history is associated with this new velocity. The physical motivation for the new procedures to assign a value to a new fluid cell internal velocity

 © 1997 John Wiley & Sons, Ltd.

is the search for the value that provides the best representation of the momentum history of the fluid that has entered the cell.

The velocity normal to each face of a new fluid cell will either be a surface velocity, if the face is shared with an empty cell, or a new internal velocity, if the face is shared with a surface or full cell. All four velocities associated with each new fluid cell represent field variables in the present computational cycle. A velocity associated with the face of a new fluid cell may have been a surface velocity with a specific value at the start of the computational cycle. If, however, the face of the new fluid cell was shared with another empty cell prior to marker movement, the velocity associated with the face was an unknown quantity at the start of the computational cycle. In this section, new procedures for the assignment of tentative values to new fluid cell internal velocities are presented. Micro cells play an essential role in the new procedures.

The free surface locations before and after marker movement are sketched in Figure 8 for an example problem. Before marker movement, cells (i, j) and $(i+1, j)$ both are empty cells, while after marker movement, these same two cells both are new surface cells. Attention will be focused on the four velocities associated with new fluid cell (i, j). After marker movement, $\tilde{v}_{i,j-1}$ is a new surface velocity, while $\tilde{u}_{i-1,j}$, $\tilde{u}_{i,j}$ and $\tilde{v}_{i,j}$ all are new internal velocities that must be assigned tentative values. Before marker movement, cell (i, j) was an empty cell that had two surface and two empty neighbours. Therefore at $t = t_0$ the velocities $v_{i,j}$ and $u_{i-1,j}$ are surface velocities that are known, while the velocities on the other two faces are unknown. The tentative values of the new internal velocities $\tilde{v}_{i,j}$ and $\tilde{u}_{i-1,j}$ are simply assigned the values of the surface velocities at the same locations at the start of the computational cycle. However, since no value of $u_{i,j}$ is available at the start of the computational cycle, another procedure must be devised to assign a physically meaningful tentative value to the new internal velocity $\tilde{u}_{i,j}$.

Three different procedures for the assignment of new fluid cell internal velocities have been developed for marker and cell methods. In the MAC method the initial value of any new internal velocity is taken to be the average of the appropriate components of the velocities of the markers that have entered the new fluid cell. Therefore the values assigned to new internal velocities in the MAC method depend on the direction of cell sweeping. In the simplified marker and cell (SMAC) method[8] a new internal velocity is initialized immediately after the first marker enters the cell. The value assigned to the new internal velocity is obtained from the cell from which the first marker came. As a consequence, the values assigned to new internal velocities in the SMAC method depend on the order of marker sequencing. In Reference 5 it is pointed out that both the MAC and SMAC procedures for the assignment of new internal velocities artificially introduce asymmetry and an alternative procedure is introduced.

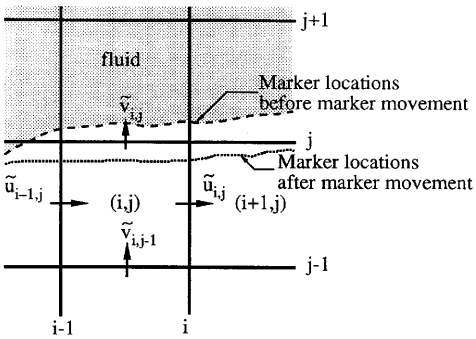

Figure 8. New fluid cells (i, j) and $(i+1, j)$

© 1997 John Wiley & Sons, Ltd.

The procedure of Reference 5 is efficient and, in contrast with the MAC and SMAC procedures, is unconditionally independent of cell and marker sequencing and does not artifically introduce asymmetry. In the procedure of Reference 5 the two closest neighbour velocities of the new internal velocity are examined. If only one of them is a surface or internal velocity, the new internal velocity is assigned the value of this neighbour velocity. If both of them are surface or internal velocities, the new internal velocity is assigned the average of the two closest neighbour velocities. This latter condition will occur when fluid fronts converge. Although there is no way to tell by use of standard finite difference cells alone, it is possible that only one of the two neighbour velocities is related to the momentum flux into the cells associated with the new internal velocity. The use of micro cells allows one to distinguish between the two neighbour velocities in such a situation. In the following a new procedure is presented that improves the accuracy of the assignment of new internal velocities in situations that occur when fluid fronts converge.

In the new procedure the momentum flux is taken into account by checking the condition of certain micro cells. In Figure 9, cells (i, j) and $(i+1, j)$ are new fluid cells and $\tilde{u}_{i,j}$ is a new internal velocity. Since cells (i, j) and $(i+1, j)$ were empty at the start of the cycle and the time increment is always chosen such that fluid does not move in either the x-or the y-direction in one time step a distance larger than the dimension of a micro celll, only the shaded micro cells in cells (i, j) and $(i+1, j)$ can contain fluid. By examining these shaded micro cells and the local velocity field, one can determine the origin of the fluid that has entered cells (i, j) and $(i+1, j)$.

Eight neighbour velocities of $\tilde{u}_{i,j}$, namely $\tilde{u}_{i+1,j}$, $\tilde{u}_{i,j+1}$, $\tilde{u}_{i-1,j}$, $\tilde{u}_{i,j-1}$, $\tilde{u}_{i+1,j+1}$, $\tilde{u}_{i-1,j+1}$, $\tilde{u}_{i-1,j-1}$ and $\tilde{u}_{i+1,j-1}$, are shown in Figure 9. The problem is to identify each neighbour velocity that is associated with the momentum flux into the cells associated with $\tilde{u}_{i,j}$ and therefore is physically relevant to the assignment of the tentative new internal velocity $\tilde{u}_{i,j}$. For this example the micro cells in the cells (i, j) and $(i+1, j)$ are numbered from left to right and bottom to top, starting with micro cell (i_1, j_1) in the lower left corner of cell (i, j) and ending with micro cell (i_6, j_3) in the top right corner of cell $(i+1, j)$. The assignment of $\tilde{u}_{i,j}$ is accomplished by the following three hierarchical steps.

Step 1

If any of the four micro cells (i_2, j_1), (i_3, j_1), (i_4, j_1) and (i_5, j_1) are surface cells, then fluid must have entered the control volume for $\tilde{u}_{i,j}$ from below, from one or both of cells $(i, j-1)$ and $(i+1, j-1)$. Therefore $\tilde{u}_{i,j-1}$ was an internal velocity at $t=t_0$ and it is the appropriate x-direction donor velocity for the momentum flux across the bottom face of the control volume for $\tilde{u}_{i,j}$. Similarly, if any of the four micro cells (i_2, j_3), (i_3, j_3), (i_4, j_3) and (i_5, j_3) are surface cells, then fluid must have

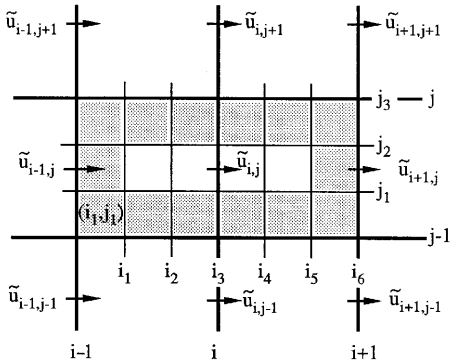

Figure 9. Assignment of tentative value to new fluid cell internal velocity $\tilde{u}_{i,j}$

 © 1997 John Wiley & Sons, Ltd.

entered the control volume for $\tilde{u}_{i,j}$ from above. If so, then $\tilde{u}_{i,j+1}$ was an internal velocity at $t = t_0$ and it is the appropriate x-direction donor velocity for the momentum flux across the top face of the control volume for $\tilde{u}_{i,j}$.

If fluid has entered the control volume for $\tilde{u}_{i,j}$, both from below and above, then $\tilde{u}_{i,j} = (\tilde{u}_{i,j-1} + \tilde{u}_{i,j+1})/2$. If fluid has entered only from below or above, then either $\tilde{u}_{i,j} = \tilde{u}_{i,j-1}$ or $\tilde{u}_{i,j} = \tilde{u}_{i,j+1}$. If all eight macro cells considered in Step 1 are empty, then Step 2 is carried out.

Step 2

If micro cell (i_1, j_2) is a surface cell, then fluid must have entered it from cell $(i - 1, j)$ and $\tilde{u}_{i-1,j}$ is the appropriate x-direction donor velocity for the momentum flux into cell (i, j). Similarly, if micro cell (i_6, j_2) is a surface cell, then $\tilde{u}_{i+1,j}$ is the appropriate x-direction donor velocity for the momentum flux into cell $(i+1, j)$.

If micro cells (i_1, j_2) and (i_6, j_2) are both surface micro cells, then fluid is approaching the control volume for $\tilde{u}_{i,j}$ from both the left and the right and the best estimate of the tentative new internal velocity is $\tilde{u}_{i,j} = (\tilde{u}_{i-1,j} + \tilde{u}_{i+1,j})/2$. If only one of micro cells (i_1, j_2) and (i_6, j_2) is a surface cell, then either $\tilde{u}_{i,j} = \tilde{u}_{i-1,j}$ or $\tilde{u}_{i,j} = \tilde{u}_{i+1,j}$. If neither micro cell (i_1, j_2) nor micro cell (i_6, j_2) is a surface cell, then Step 3 is carried out.

Step 3

The only remaining possibility is that fluid has entered at least one of micro cells (i_1, j_1) and (i_1, j_3) in cell (i, j) and at least one of micro cells (i_6, j_1) and (i_6, j_3) in cell $(i+1, j)$.

If micro cell (i_1, j_1) is a surface cell, then fluid may have entered it from cell (i, j). If so, then cell (i, j) must have contained fluid at the start of the cycle and $\tilde{u}_{i-1,j}$ is the most appropriate x-direction donor velocity for the momentum flux into micro cell (i_1, j_1). Therefore, if cell $(i - 1, j)$ was a surface cell at the start of the cycle, then $\tilde{u}_{i-1,j}$ is used in the assignment of the tentative new internal velocity $\tilde{u}_{i,j}$. On the other hand, if cell $(i - 1, j)$ was empty at the start of the cycle, then one or both of cells $(i - 1, j - 1)$ and $(i, j - 1)$ must have contained fluid at the start of the cycle. Otherwise, fluid could not have entered micro cell (i_1, j_1). In this case, regardless of whether one or both of cells $(i - 1, j - 1)$ and $(i, j - 1)$ contained fluid, $\tilde{u}_{i-1,j-1}$ is the most appropriate x-direction donor velocity for the momentum flux into micro cell (i_1, j_1).

In a similar manner the most appropriate x-direction donor velocity is determined for the momentum flux into each of the other three micro cells (i_1, j_3), (i_6, j_1) and (i_6, j_3) that is a surface cell. Finally, the most physically meaningful estimate of the tentative new internal velocity $\tilde{u}_{i,j}$ is the average value of the x-direction donor velocities associated with all four micro cells (i_1, j_1), (i_1, j_3), (i_6, j_1) and (i_6, j_3) that contain fluid.

For example, if micro cells (i_1, j_1) and (i_6, j_3) are the only surface cells and fluid enters micro cell (i_1, j_1) from below and micro cell (i_6, j_3) from above (cells $(i - 1, j)$ and $(i+2, j)$ contained no fluid at the start of the cycle), then $\tilde{u}_{i,j} = (\tilde{u}_{i-1,j-1} + \tilde{u}_{i+1,j+1})/2$.

The order of Steps 1–3 is important. Suppose, for example, that there is fluid only in micro cells (i_3, j_1) and (i_1, j_2). Cell (i_3, j_1) is located inside the conntrol volume for $\tilde{u}_{i,j}$, while cell (i_1, j_2) is located just outside the control volume. Therefore $\tilde{u}_{i,j-1}$, the appropriate x-direction donor velocity for micro cell (i_3, j_1), is a more physically meaningful estimate for the tentative new internal velocity $\tilde{u}_{i,j}$ than $\tilde{u}_{i-1,j}$, the appropriate x-direction donor velocity for micro cell (i_1, j_2). In the new procedure, $\tilde{u}_{i,j}$ would be assigned the value of $\tilde{u}_{i,j-1}$ in Step 1 above. If Steps 1 and 2 were reversed, $\tilde{u}_{i,j}$ would instead be incorrectly assigned the value of $\tilde{u}_{i-1,j}$.

© 1997 John Wiley & Sons, Ltd.

6. THE PRESSURE FIELD

The new pressure equation used in the SMMC method is derived starting from the Navier–Stokes equation written in terms of the final velocities, the tentative velocities and the pressure:

$$\frac{\partial u}{\partial t} = \frac{\partial \tilde{u}}{\partial t} - \frac{1}{\rho}\frac{\partial p}{\partial x}, \qquad \frac{\partial v}{\partial t} = \frac{\partial \tilde{v}}{\partial t} - \frac{1}{\rho}\frac{\partial p}{\partial y}. \tag{10}$$

Integrating equation (10) with respect to time from t to $t+\delta t$ leads to

$$u = \tilde{u} - \frac{\delta t}{\rho}\frac{\partial p}{\partial x}, \qquad v = \tilde{v} - \frac{\delta t}{\rho}\frac{\partial p}{\partial y}. \tag{11}$$

Then the procedure described in the development of the pressure potential equation recently presented in Reference 9 is followed. Namely, equation (11) are written in second-order central difference form for a generic cell and then substituted into the second-order central difference form of the continuity equation for the control volume associated with that cell. The result is the pressure Poisson equation

$$Cp - \frac{1}{\delta x\, le}pe - \frac{1}{\delta x\, ln}pn - \frac{1}{\delta x\, lw}pw - \frac{1}{\delta x\, ls}ps = -\frac{\rho}{\delta t}D \tag{12}$$

for the discrete pressure p at the centre of cell (i, j), where

$$C = \frac{1}{\delta x}\left(\frac{1}{le}+\frac{1}{lw}\right) + \frac{1}{\delta y}\left(\frac{1}{ln}+\frac{1}{ls}\right), \qquad D = \frac{\tilde{u}(i, j) - \tilde{u}(i-1, j)}{\delta x} + \frac{\tilde{v}(i, j) - \tilde{v}(i, j-1)}{\delta y},$$

pe, pn, pw and ps represent the pressures at points e, n, w and s respectively and le, ln, lw and ls represent the leg lengths for cell (i, j). Points e, w, n and s are points at which either the pressure is calculated or a pressure boundary condition is applied. The preconditioned conjugate gradient method is used to solve equation (12). Iterations continue until the change in the value of any pressure is less than a user-specified convergence criterion.

In previous methods the pressure boundary conditions, as originally suggested in the MAC method, are split into two parts that are applied in different stages of the computational cycle. Previous treatments of certain free surface velocity boundary conditions have a destabilizing influence on the numerical solution. In previous methods those parts of the pressure boundary conditions related to the viscous normal stresses and the applied pressure at the free surfaces, along with an artificially high value of the viscosity, are applied as pseudopressures during the calculation of the tentative velocities, which has the effect of stabilizing the solution. The other pressure boundary conditions, together with the assumption of zero pressuree at the free surfaces, are then applied in conjunction with the calculation of the pressure potential field. Treatments of free surface velocity boundary conditions which eliminate the destabilizing influences of previous treatments were presented in Reference 5 and are incorporated in the new method of this paper. Consequently, in the SMMC method it is possible to take into account all the pressure boundary conditions during the calculation of the pressure field, including the impact pressure boundary conditions introduced in Reference 9. No pressure boundary condition nor any other pressure value is taken into account during the calculation of the tentative velocity field. As a result, the final pressure field, including all the pressure boundary conditions, is associated with the tentative velocity field calculated in the current computational cycle. In previous methods, however, some of the pressure boundary conditions are associated with the final velocity field of the previous cycle, while others are associated with the tentative velocity field of the current cycle.

In the MAC method, three symbols ϕ, θ and ψ are used that are related to pressure. The symbol ϕ is referred to as the 'true pressure' and is equal to the pressure divided by the density, the symbol θ is

 © 1997 John Wiley & Sons, Ltd.

referred to as the 'pseudopressure' and ψ is simply referred to as a 'potential'. The relationship between ϕ, θ and ψ is

$$\phi = \theta + \psi/\delta t.$$

The pseudopressure θ is based on the final velocity field of the previous cycle, while the potential ψ is based on the tentative velocity field of the current cycle.

In the SMMC method the pressure is designated by p, no pseudopressure or potential is referenced at all, all pressure boundary conditions are applied during the solution of the new pressure equation and the pressure and velocities all are associated with the same instant of time.

7. FINAL VELOCITIES

After the pressure field has been calculated by use of (12), the final velocities are determined. The use of micro cells enables the recognition and accommodation of four essentially different cases for the determination of final internal velocity components. For the cases illustrated in Figure 10, $u(i, j)$ is the final velocity to be determined. Corresponding to each case shown in Figure 10, there also is a case for which $v(i, j)$ is the final velocity to be determined.

For the first case shown in Figure 10(a), $u(i, j)$ is immersed in the fluid and a free surface exists in the cell to the right (east) of cell (i, j). In this case, $le(i, j)$ is larger than $\delta x/2$ and the final velocity $u(i, j)$ is computed by use of

$$u(i, j) = \tilde{u}(i, j) - \frac{\delta t}{\rho} \frac{pe(i, j) - p(i, j)}{le(i, j)}. \tag{13}$$

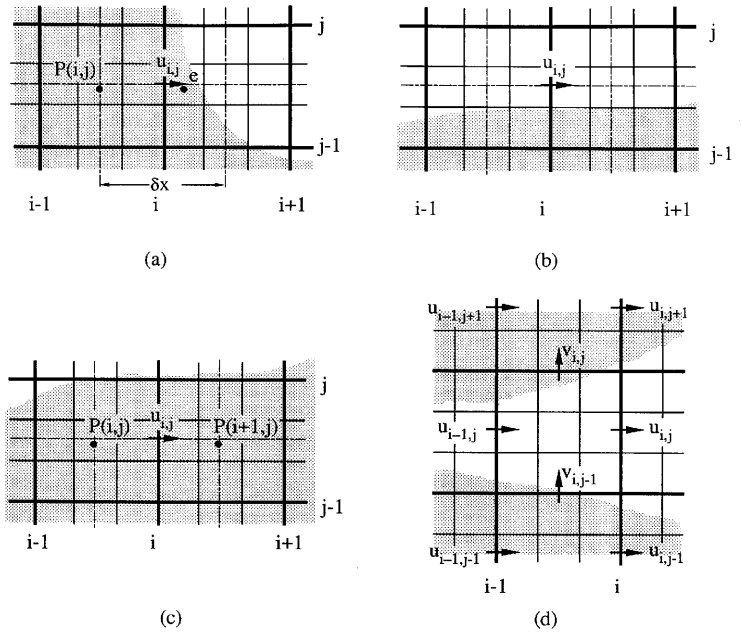

Figure 10. Final velocities

© 1997 John Wiley & Sons, Ltd.

Point e, the centre of the surface micro cell to the east of $u(i, j)$, represents a point on the free surface, $pe(i, j)$ is the pressure on the free surface and $le(i, j)$ is the distance between the centre of cell (i, j) and point e.

In the second case shown in Figure 10(b), $u(i, j)$ is an internal velocity associated with a face between two surface cells, but it actually is located outside the fluid. In this case neither $le(i, j)$ nor $lw(i+1, j)$ is larger than $\delta x/2$, no pressure gradient is available for the adjustment of $\tilde{u}(i, j)$ and the final velocity $u(i, j)$ is simply assigned the value of $u(i, j-1)$, the closest appropriate neighbour velocity.

For the third case shown in Figure 10(c), the velocity $u(i, j)$, the centre of cell (i, j) and the centre of cell $(i+1, j)$ are all within the fluid. Equation (14) applies for this case, which represents the most common case for an internal velocity:

$$u(i, j) = \tilde{u}(i, j) - \frac{\delta t}{\rho} \frac{p(i+1, j) - p(i, j)}{\delta x}. \tag{14}$$

The fourth case shown in Figure 10(d) occurs when free surfaces converge. The final values assigned to the velocities $u(i-1, j)$ and $u(i, j)$ shown in Figure 10(d) are related to the motions of both of the two converging fluid fronts. The velocity $u(i-1, j)$ is assigned the average value of $u(i-1, j+1)$ and $u(i-1, j-1)$, while $u(i, j)$ is assigned the average value of $u(i, j+1)$ and $u(i, j-1)$. If the fluid fronts converge during the next computational cycle, these values will be used for the calculation of the incompressibility deviation $D(i, j)$ and the subsequent calculation of $p(i, j)$. Otherwise, these values of $u(i-1, j)$ and $u(i, j)$ will never be used at all. When values of $u(i-1, j)$ and $u(i, j)$ are needed in the next computational cycle for moving surface markers or calculating tentative velocities, physically appropriate values are determined and used as needed but are not stored.

After all the final internal velocities have been determined, the required final velocity boundary conditions must be determined. Since outside tangential velocities are not stored in the SMMC method, the final surface velocities are the only final velocity boundary conditions that must be determined. Except for the special case of converging fluid fronts illustrated by the surface velocity $u(i, j)$ shown in Figure 10(d) and discussed above, the final surface velocity assignment procedures presented in Reference 5 are adopted in the SMMC method.

8. CONVERGING FLUID FRONTS AND MULTIVALUED VELOCITIES

Since spatial derivatives are approximated by second-order central differences and an explicit method is employed to evolve the solution, a marker and cell method has second-order accuracy in space and first-order accuracy in time. The cell dimensions δx and δy are the measures of spatial resolution and the time increment δt is the measure of temporal resolution.

In previous methods the spatial resolution in the vicinity of converging fluid fronts is not equal to the cell spacing and can be as coarse as twice the cell spacing. Consequently, the spatial resolution and accuracy of previous methods are significantly less in the neighbourhood of converging fluid fronts than elsewhere in the computational domain.

In the SMMC method there is no degradation of spatial resolution or loss of spatial accuracy in connection with converging fluid fronts. This improvement is enabled by use of micro cells, as illustrated in Figure 11. Two fluid fronts separated by slightly less than twice the cell spacing are shown in Figure 11(a). In previous methods, in spite of the fact that the fluid fronts are separated by almost twice the cell spacing, both of the cells in the centre of Figure 11(a) are flagged as full cells, since neither of them has an empty neighbour. The same situation is depicted in Figure 11(b), except that micro cells have been added, enabling the ready identification of the two distinct fluid fronts and

 © 1997 John Wiley & Sons, Ltd.

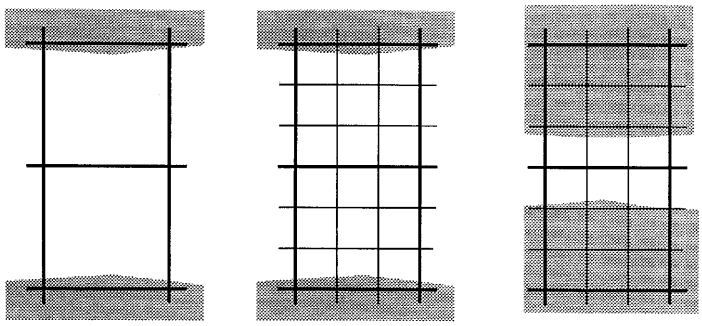

Figure 12. Experimental apparatus

of the empty region between them. With micro cells the gap between the two fronts is identifiable until fewer than two micro cells separate them, as shown in Figure 11(c). Consequently, in the SMMC method the spatial resolution is not degraded in connection with converging fluid fronts and, in conjunction with the use of multivalued velocities, second-order accuracy in space is maintained.

In the new method the physical purpose for which the velocity is required is taken into account in order to assign appropriate values to velocities between converging fluid fronts.

For marker movement and the calculation of tentative velocities the velocities $u(i-1, j)$ and $u(i, j)$ of the typical example of converging fluid fronts shown in Figure 10(d) should be assigned values that are related to the motion of the upper fluid front when that part of the fluid is under consideration. On the other hand, when the lower part of the fluid is under consideration, the same two velocities instead should be assigned values that are related to the motion of the lower fluid front. Essentially, one fluid front should be ignored when the motion of the other is under consideration. This is a crucial point in the treatment of converging fluid fronts. For example, if, as in previous methods, no special consideration is given to the typical situation involving converging fluid fronts that is illustrated in Figure 10(d), the velocity $u(i, j)$ is simply regarded as the single surface velocity associated with a surface cell that has only one empty neighbour. Then the value of $u(i, j)$ is computed by use of the discrete continuity equation associated with cell (i, j). As a consequence, the velocities $u(i-1, j)$, $v(i, j)$ and $v(i, j-1)$ all directly influence the value of $u(i, j)$ and $D(i, j)$ is equal to zero. Since $v(i, j)$ is associated with the upper fluid front, while $v(i, j-1)$ is associated with the lower fluid front, this procedure allows each fluid front to begin to affect the other before they actually converge. In addition, when the fronts converge, it is not possible to compute the increase in pressure in cell (i, j), because the incompressibility deviation $D(i, j)$ in cell (i, j) is equal to zero.

In the new method, velocities such as $u(i-1, j)$ and $u(i, j)$ in Figure 10(d) are assigned values in the new method for five different purposes during the current computational cycle. They are assigned values (i) for movement of markers associated with the upper fluid front, (ii) for calculation of tentative velocities associated with the upper fluid front, (iii) for movement of markers associated with the lower fluid front, (iv) for calculation of tentative velocities associated with the lower fluid front and (v) for calculation of the incompressibility deviation and the pressure in cell (i, j) in case the fronts converge during the current cycle.

When the upper part of the fluid is under consideration and the lower fluid front in Figure 10(d) is temporarily ignored, cell $(i-1, j)$ appears to be a surface cell with one empty neighbour below and cell (i, j) appears to be a surface cell with two adjacent empty neighbours below and to the right. Therefore, for movement of the upper fluid front, $u(i-1, j)$ is recognized as an internal velocity of

© 1997 John Wiley & Sons, Ltd.

the type shown in Figure 10(b) and therefore is assigned the value of $u(i-1, j+1)$. To satisfy continuity in cell (i, j), the surface velocity $u(i, j)$ then is assigned the value of $u(i-1, j)$. For the calculation of tentative internal velocities associated with the upper part of the fluid, $u(i-1, j)$ again is assigned the value of $u(i-1, j+1)$, but $u(i, j)$ instead is assigned the value of $u(i, j+1)$, the closest appropriate fluid velocity.

On the other hand, when the lower part of the fluid is under consideration and the upper fluid front is temporarily ignored, cell $(i-1, j)$ appears to be a surface cell with one empty neighbour above and cell (i, j) appears to be a surface cell with two adjacent empty neighbours above and to the right. As a consequence, $u(i-1, j)$ and $u(i, j)$ both are assigned the value of $u(i-1, j-1)$ for movement of the lower fluid front. For calculation of tentative internal velocities associated with the lower part of the fluid, $u(i-1, j)$ is also assigned the value of $u(i-1, j-1)$, while $u(i, j)$ instead is assigned the value of $u(i, j-1)$.

Finally, for the calculation of the incompressibility deviation $D(i, j)$ and the subsequent calculation of the pressure $p(i, j)$ in case the fronts converge, $u(i-1, j)$ and $u(i, j)$ are assigned values that are related to the motions of both of the two converging fluid fronts; $u(i-1, j)$ is assigned the average value of $u(i-1, j+1)$ and $u(i-1, j-1)$, while $u(i, j)$ is assigned the average value of $u(i, j+1)$ and $u(i, j-1)$. These values of $u(i-1, j)$ and $u(i, j)$ will not be used at all unless the fluid fronts converge.

In summary, for the situation shown in Figure 10(d), the velocity $u(i-1, j)$ is assigned the value of $u(i-1, j+1)$ for purposes (i) and (ii), the value of $u(i-1, j-1)$ for purposes (iii) and (iv) and the average value of $u(i-1, j+1)$ and $u(i-1, j-1)$ for purpose (v). Therefore three distinct values are actually assigned to $u(i-1, j)$ during the current cycle. For $u(i, j)$, on the other hand, five different values are assigned during the current cycle. For purpose (i), $u(i, j) = u(i-1, j) = u(i-1, j+1)$; for purpose (ii), $u(i, j) = u(i, j+1)$; for purpose (iii), $u(i, j) = u(i-1, j) = u(i-1, j-1)$; for purpose (iv), $u(i, j) = u(i, j-1)$; and for purpose (v), $u(i, j)$ is assigned the average value of $u(i, j+1)$ and $u(i, j-1)$.

The first advantage of the use of multivalued velocities for the special case of converging fluid fronts is that the velocities used at different points in the computational cycle are physically appropriate for the purpose under consideration and do not incorrectly allow the fronts to begin to affect each other as they approach each other and before they actually converge. The second, equally important, advantage of the use of multivalued velocities is that values that capture the motions of both fluid fronts are available in case the fronts actually converge. These values then allow the calculation of an appropriate non-zero value of $D(i, j)$, which enables the evaluation of the increase in pressure in cell (i, j) that occurs as a result of the convergence of the two fronts.

9. EXPERIMENTAL VALIDATION

To demonstrate both the capabilities and the validity of the SMMC method, simulation and experimental results are compared for water sloshing in a tank. No previous method is capable of simulating free surface fluid flow that includes impact and converging fluid fronts. To obtain the experimental results, a partially filled tank with clear glass walls is placed on a platform with wheels. The tank is caused to move horizontally back and forth in a periodic fashion by use of a constant speed electric motor, a crank and a connecting rod between the crank and the platform. As a result of the motion of the tank, the water, which initially is at rest, sloshes back and forth inside the tank. A high-speed video camera is used to capture, at 500 frames per second, the primarily two-dimensional motion of the fluid in the tank. A sketch of the experimental apparatus is found in Figure 12.

Direct comparisons between simulation and experimental results at 16 different times during the first two cycles of the tank's motion can be made by examination of Figure 13. For each of the 16

 © 1997 John Wiley & Sons, Ltd.

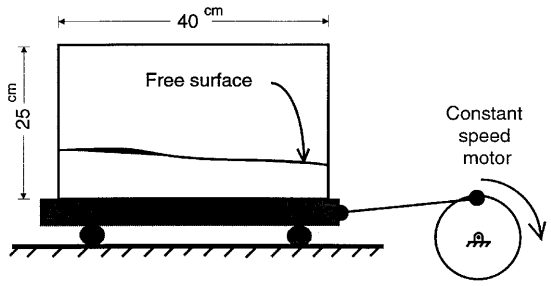

Figure 12. Experimental apparatus

times a pair of figures is displayed in Figure 13. One of the two figures in each pair depicts the SMMC simulation result, with the shape and location of the free surface at the instant in question clearly identified by surface markers. The other figure in each pair is a video image of the experiment at the same instant. In the video image the shape and location of the free surface are visible through the transparent wall of the tank. Since the camera is stationary while the tank moves back and forth, the tank does not occupy exactly the same position in the camera's field of view at each of the 16 times. The effects of these differences in position are inconsequential, since the tank only moves

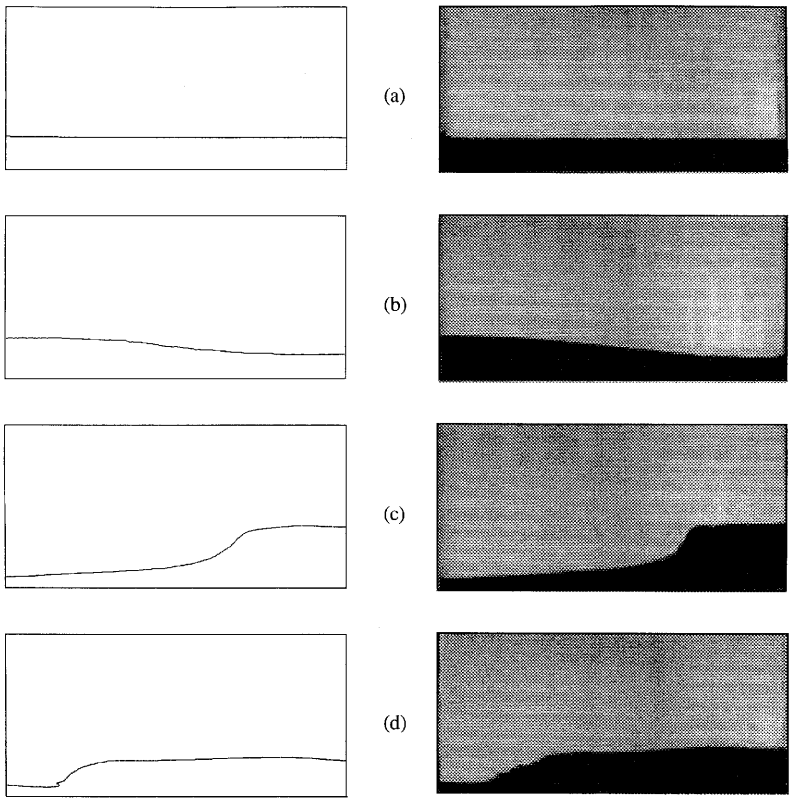

Figure 13. SMMC simulation and experimental results for water sloshing in a tank

© 1997 John Wiley & Sons, Ltd.

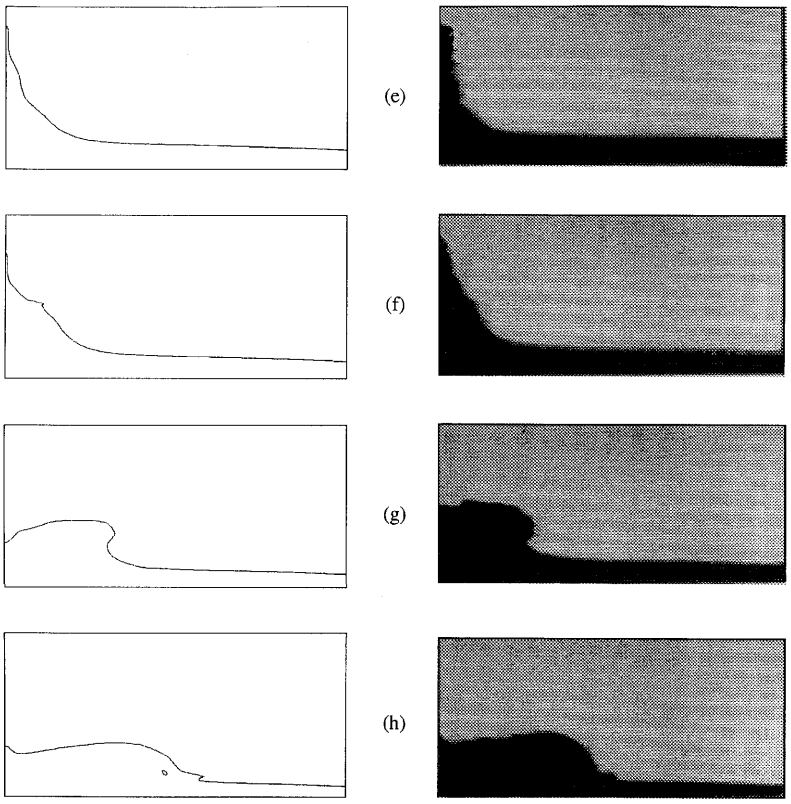

Figure 13. (*continued*)

15 cm to either side of its central location and the camera lens is located 9 m from the tank. The most significant effect occurs when the tank is in an extreme position and a thin layer of fluid has run up its end wall. In this case the thickness of the layer extending across the end wall is exaggerated to some extent as a result of the fact that the thin layer of fluid is to one side of the line of sight of the camera.

The most violent sloshing occurs during the first two cycles of the back and forth motion of the tank. General inspection of Figures 13(a)–13(p) leads one to conclude that the simulated free surface shapes and locations are in good agreement with their experimental counterparts throughout these first two complete cycles of the tank's motion. The initial depth of the water in the tank is 4 cm. The period of the motion of the tank is 1·70 s and the times associated with the pairs of figures range from 0·05 to 3·45 s. The 40 cm $\times$ 20 cm computational domain was divided into 160×80 macro cells, each 0·25 cm $\times$ 0·25 cm, and nine micro cells were used per macro cell ($N = 3$). A variable time step is used in the SMMC simulation and 3741 computational cycles were completed in reaching the real time of 3·45 s. The simulation was performed on a DEC 5000/260 workstation and required 10,677 s of computer time. In the succeeding paragraphs a brief discussion of the details of the sloshing motion and of the relationship between simulated and experimental results is presented.

In Figure 13(a), just 0·05 s after the tank begins to move to the right, the surface of the fluid is still nearly horizontal, although a slight build-up of fluid near the left end of the tank is visible. At 0·55 s the build-up of fluid in the left half of the tank is clearly apparent in Figure 13(b) The first half-cycle of the tank's motion is completed at 0·85 s, at which time motion to the right ceases and motion to the

 © 1997 John Wiley & Sons, Ltd.

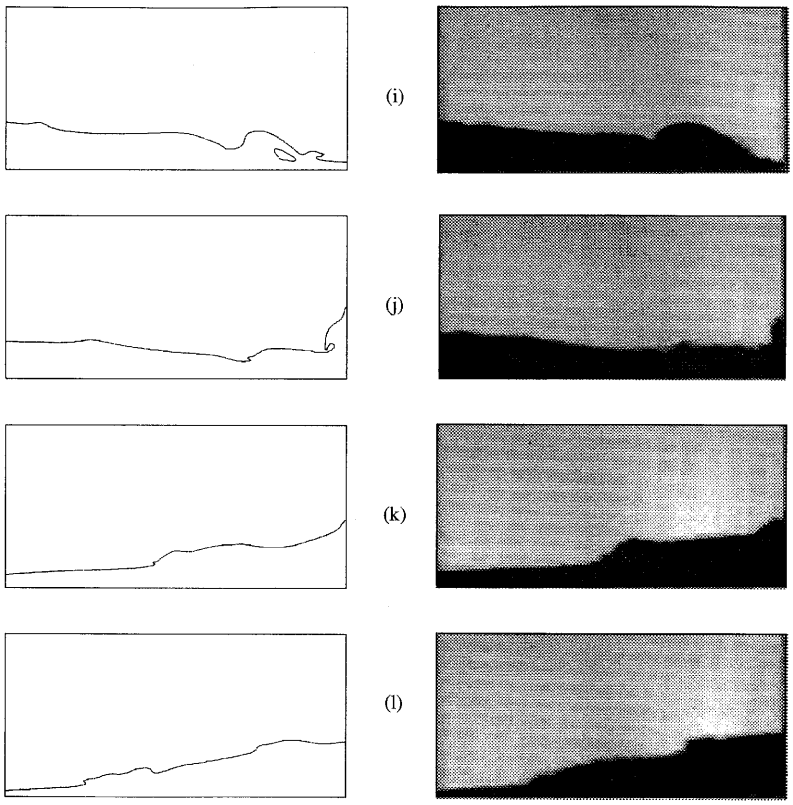

Figure 13. (*continued*)

left is impending. At 1·10 s, as shown in Figure 13(c), the tank has moved part way back to the left and fluid has accumulated in the right end of the tank. In Figure 13(d) the tank is still moving to the left and the upper portion of the fluid is moving to the left with a speed greater than that of the tank. The shapes and locations of the simulated and experimental fluid fronts are essentially the same in Figures 13(a)–13(d). Up to this point in time the motion of the fluid is relatively smooth, no impact has occurred and the free surface can be represented as single-valued. Before the end of the first cycle of the tank's motion, however, the fluid impacts the left end of the tank and moves dramatically up the left tank wall, as shown in Figure 13(e). At 1·70 s the first cycle is completed, leftward motion of the tank ceases and motion back to the right impends. A breaking wave moving to the right is visible in Figure 13(g), just 0·05 s after the tank has resumed motion to the right. Even though impact with the end wall of the tank has occurred and the shape of the free surface is multivalued, the agreement between simulated and experimental results remains excellent. Between 1·75 and 1·85 s the breaking wave collapses. Following this convergence of fluid fronts, the agreement between simulated and experimental results is still very good, as shown in Figure 13(h).

A small void is apparent in the simulation results shown in Figure 13(h). Voids also are apparent in Figures 13(i) and 13(o). These voids are the result of the convergence of fluid fronts during wave breaking in such a manner that empty regions become completely surrounded by fluid. The falling fluid shown in the breaking wave near the right end of the tank in Figure 13(j) is just about to converge with the fluid below and completely surround a small region that contains no fluid. In the

© 1997 John Wiley & Sons, Ltd.

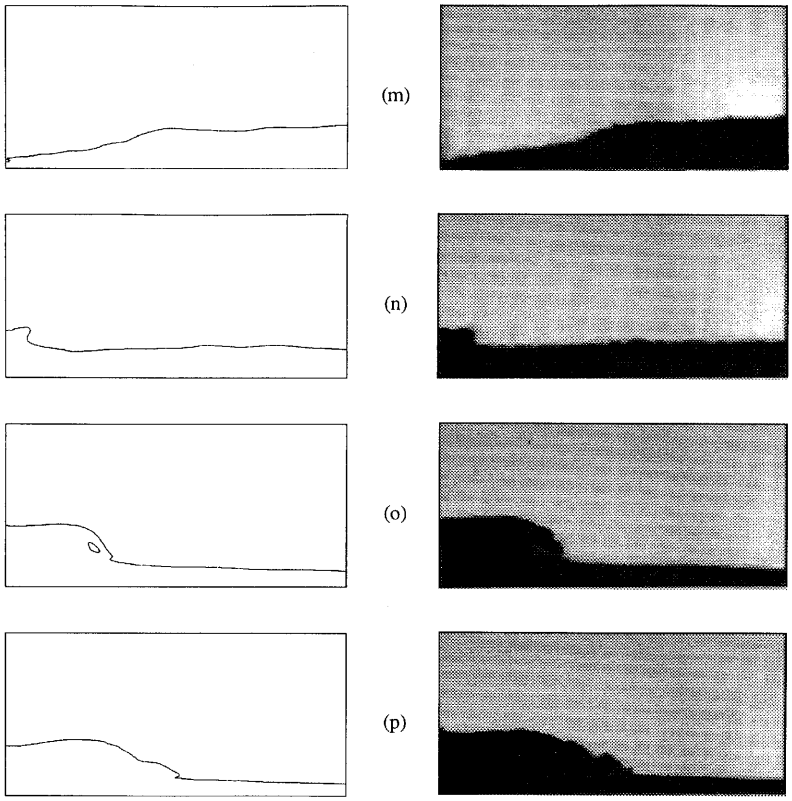

Figure 13. (*continued*)

simulation such voids eventually close and disappear. In the actual physical occurrence of a breaking wave, air is temporarily entrapped inside the fluid. It is not possible to observe any air entrapment in the video images of the experiment, because the camera sees through the glass wall and the fluid and cannot display just one isolated two-dimensional vertical slice at some point between the side walls.

Repeated occurrences of impact and of the convergence of fluid fronts take place during the simulation of the first two cycles of the tank's motion. Nevertheless, the results displayed in Figures 13(e)–13(p), all of which are subsequent to one or more occurrences of impact and/or fluid front convergence, continue to exhibit good agreement between the shapes and locations of the simulated and experimental free surfaces.

10. GRID REFINEMENT STUDY

Four different simulations of the water-sloshing problem considered in the previous section are compared with each other to demonstrate the convergence of the new method. The macro cell size is different for each of the four cases. Otherwise, the cases are identical. For Case 1 the computational domain is divided into only 40×20 macro cells, each 1 cm $\times$ 1 cm. The macro cell dimension is halved for Case 2, halved again for Case 3 and halved still again for Case 4. Therefore there are four times as many cells in each successive case. The finest grid, the one used in Case 4, has 64 times as many cells as the coarsest grid, the one used in Case 1. The grid spacing for Case 3 is the same as for

 © 1997 John Wiley & Sons, Ltd.

Table I. Data for grid refinement study

Case	I_x	I_y	δx (cm)	δy (cm)	CPU time (s)
1	40	20	1·0	1·0	48·3
2	80	40	0·5	0·5	286·7
3	160	80	0·25	0·25	3115·2
4	320	160	0·125	0·125	31009·9

the simulation results presented in the previous section; namely, the domain is divided into 160×80 cells, each $0{\cdot}25$ cm $\times\, 0{\cdot}25$ cm.

Data for the four cases are presented in Table I, where I_x and I_y represent the numbers of cells in the x-and the y-direction respectively and δx and δy are the cell dimensions. The last column in Table I presents the DEC 5000/260 CPU time consumed by each simulation. For each case the simulation was terminated at $t = 1{\cdot}101$ s, the time that corresponds to Figure 13(c).

The simulation results for all four cases are displayed in Figure 14. In the inset in Figure 14 the entire computational domain is displayed. At this resolution the differences between the four cases are indiscernible. In order to differentiate between the four cases, the portion of the free surface enclosed by the small rectangular window in the inset is enlarged and displayed in the large rectangle. The legends associated with the different curves refer to the numbers of cells in the x-and the y-direction for the four cases.

It is apparent from close examination of Figure 14 that the solution converges as the grid density is increased. The difference between Case 1 and Case 4 is greater than that between Case 2 and Case 4, which itself is greater than the difference between Case 3 and Case 4. In addition, the change in the solution from one case to the next gets smaller and smaller as the grid density increases. Finally, comparison of the curves shown in Figure 14 with the experimental result displayed in Figure 13(c) reveals that the simulation result becomes closer to the experimental result as the grid density increases. The transition from the lower free surface level on the left to the higher level on the right becomes steeper as the grid density increases.

It can be concluded that the solution provided by the new method converges as the grid density is increased and also that it gets closer to the actual experimental result. By use of the new method, even a coarse mesh with only 40×20 cells leads to a reasonably good solution of the free surface flow problem considered.

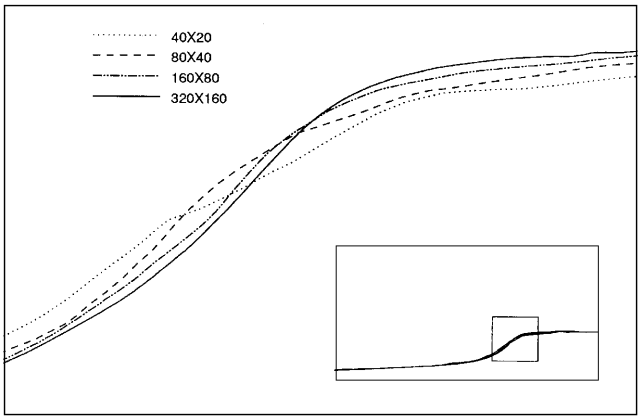

Figure 14. Simulation results for sloshing problem at $t = 1{\cdot}101$ s by use of four different grid densities

© 1997 John Wiley & Sons, Ltd.

11. CONCLUSIONS

A new method capable of simulating two-dimensional, incompressible, transient, free surface fluid flow problems that include multivalued free surfaces, impact of free surfaces with solid obstacles and converging fluid fronts is presented. The new method is validated by comparison of simulation and experimental results for water sloshing in a tank. The comparison reveals good agreement between the shapes and locations of the simulated and experimental free surfaces even after repeated occurrences of impact of the water with the tank walls and of the convergence of fluid fronts as the water sloshes back and forth in the tank. The convergence of the new method is demonstrated by a grid refinement study.

Physically motivated new procedures are introduced for the advection of the free surface as well as for the calculation of the velocity and pressure fields. Although use of these new procedures can have important consequences in connection with fluid-filled regions, their most significant advantages are associated with regions near the free surface and, in particular, in connection with the convergence of fluid fronts. Two guiding principles for the development of the new procedures are that the most appropriate available velocity information must be used for any given specific purpose and that great care must be exercised in the development of momentum flux approximations. It is recognized that for a particular discrete velocity that is associated with the convergence of two fluid fronts, as many as five different values are appropriate for different purposes during a single computational cycle. The use of surface markers and micro cells enables the identification of special circumstances such as the convergence of fluid fronts, as well as the development of efficient procedures for the assignment of velocities that are appropriate for the circumstances. Surface markers and micro cells also play a critical role in the development of new, more accurate momentum flux approximations. All the new procedures combine to produce a robust new method, the surface marker and micro cell (SMMC) method, that is capable of simulating free surface fluid flow that includes impact and converging fluid fronts.

ACKNOWLEDGEMENTS

Support for this research has been provided by the Defense Advanced Research Projects Agency of the U.S. Department of Defense as Projects 5-25084 and 5-25085 of Contract MDA09386-C-0182, the National Science Foundation under grant DDM-9114846, the J. Lindsay Embrey Professorship in Engineering and the Leadwell CNC Machines Manufacturing Corporation.

REFERENCES

1. F. H. Harlow and J. E. Welch, 'Numerical calculation of time-dependent viscous incompressible flow of fluid with free surface', *Phys. Fluid*, **8**, 2182–2189 (1965).
2. J. E. Welch, F. H. Harlow, J. P. Shannon and B. J. Daly, 'The MAC method: a computing technique for solving viscous, incompressible, transient fluid-flow problems involving free surfaces', *Los Alamos Scientific Laboratory Rep. LA-3425*, 1965.
3. S. Chen, D. B. Johnson and P. E. Raad, 'The surface marker method', in *Computational Modeling of Free and Moving Boundary Problems*, Vol. 1, *Fluid Flow*, de Gruyter, New York, 1991, pp. 223–234.
4. P. E. Raad, S. Chen and D. B. Johnson, 'The introduction of micro cells to treat pressure in free surface fluid flow problems', *J. Fluids Eng.*, **117**, 683–690 (1995).
5. S. Chen, D. B. Johnson and P. E. Raad, 'Velocity boundary conditions for the simulation of free surface fluid flow', *J. Comput. Phys.*, **116**, 262–276 (1995).
6. H. Miyata, 'Finite-difference simulation of breaking waves', *J. Comput. Phys.*, **65**, 179–214 (1986).
7. C. W. Hirt and B. D. Nichols, 'Volume of fluid (VOF) method for the dynamics of free boundaries', *J. Comput. Phys.*, **39**, 201–225 (1981).
8. A. A. Amsden and F. H. Harlow, 'The SMAC method: a numerical technique for calculating incompressible fluid flows', *Los Alamos Scientific Laboratory Rep. LA-4370*, 1970.
9. D. B. Johnson, P. E. Raad and S. Chen, 'Simulation of impacts of fluid free surfaces with solid boundaries', *Int. j. numer. methods fluids*, **19**, 153–176 (1994).

 © 1997 John Wiley & Sons, Ltd.